A scheme to polarize nuclear-spin of atoms by a sequence of short laser pulses: application to the muonium

Takashi Nakajima*

Institute of Advanced Energy, Kyoto University, Gokasho, Uji, Kyoto 611-0011, Japan

**t-nakajima@iae.kyoto-u.ac.jp*

Abstract: We theoretically show that a sequence of short laser pulses can efficiently polarize nuclear-spin of atoms/ions. This is a variant of optical pumping with an important difference that a sequence of short laser pulses is used instead of a continuous-wave laser. Such a replacement is particularly useful if the pumping wavelength is in the ultraviolet or vacuum-ultraviolet region where obtaining a continuous-wave light source with a sufficient intensity is very difficult. Because of the use of short laser pulses neither hyperfine transitions nor fine structure transitions are spectrally resolved, which is quite in contrast to the standard optical pumping scheme by a continuous-wave laser. As an example we apply the scheme to polarize the muonium (μ^+e^-, lifetime 2.2 μs), for which the pumping wavelength is 122 nm. From numerical solutions of a set of density matrix equations, we find that the use of only a single, two, and five pulses with a ps duration at the peak intensity of 2×10^8 W/cm^2 and a 5 ns time interval results in the degrees of spin-polarization of 33, 50, and 80 %, respectively, within the time scale of a few tens of ns.

OCIS codes: (140.5560) Pumping; (020.2930) Hyperfine structure.

References and links

1. D. Fick, G. Grawert, and I. M. Turkiewicz, "Nuclear physics with polarized heavy ions," Phys. Rep. **214**, 1–111 (1992).
2. W. Happer, "Optical pumping," Rev. Mod. Phys. **44**, 169–249 (1972).
3. J. T. Cusma and L. W. Anderson, "Polarization of an atomic sodium beam by laser optical pumping," Phys. Rev. A **28**, 1195–1197 (1983).
4. H. Reich and H. J. Jänsch, "Nuclear spin polarized alkali beams (Na,Li): Optical pumping with electro-optically modulated laser beam," Nucl. Instrum. Methods Phys. Res. A **288**, 349–353 (1990).
5. G. W. Schinn, X.-L. Han, and A. Gallagher, "Production and diagnosis of a highly spin-polarized Na beam," J. Opt. Soc. Am. B **8**, 169–173 (1991).
6. A. N. Zelenskii, K. Jayamanna, C. D. P. Levy, M. McDonald, R. Ruegg, and P. W. Schmor, "Optimization studies of proton polarization in the TRIUMF optically pumped polarized H^- ion source," Nucl. Instrum. Methods Phys. Res. A **334**, 285–293 (1993).
7. C. D. P. Levy, R. Baartman, J. A. Behr, R. F. Kiefl, M. Pearson, R. Poutissou, A. Hatakeyama, and Y. Hirayama, "The collinear laser beam line at ISAC," Nucl. Phys. A **746**, 206C–209C (2004).
8. A. N. Zelenskiy, S. A. Kokhanovskiy, V. M. Lobashev, N. M. Sobolevskiy, and E. A. Volferts, "A method of polarizing relativistic proton beams by laser radiation," Nucl. Instrum. Methods **227**, 429–433 (1984).
9. G. D. Cates, D. R. Benton, M. Gatzke, W. Happer, K. C. Hasson, and N. R. Newbury, "Laser production of large nuclear-spin polarization in frozen xenon,'" Phys. Rev. Lett. **65**, 2591–2594 (1990).
10. B. Clasie, C. Crawford, J. Seely, W. Xu, D. Dutta, and H. Gao, "Laser-driven target of high-density nuclear-polarized hydrogen gas," Phys. Rev. A **73**, 020703 (2006).

#135117 - $15.00 USD Received 14 Sep 2010; revised 2 Nov 2010; accepted 9 Dec 2010; published 14 Dec 2010

11. R. Mahon, T. J. McIlrath, and D. Koopman, "Nonlinear generation of Lyman-alpha radiation," Appl. Phys. Lett. **33**, 305–307 (1978).
12. D. Cotter, "Tunable narrow-band coherent VUV source for the Lyman-alpha region," Opt. Commun. **31**, 397–400 (1979).
13. R. Wallenstein, "Generation of narrowband tunable VUV radiation at the Lyman-α wavelength," Opt. Commun. **33**, 119–122 (1980).
14. G. Hilber, A. Lago, and R. Wallenstein, "Broadly tunable vacuum-ultraviolet/extreme-ultraviolet radiation generated by resonant third-order frequency conversion in krypton," J. Opt. Soc. Am. B **4**, 1753–1764 (1987).
15. J. P. Marangos, N. Shen, H. Ma, M. H. R. Hutchinson, and J. P. Connerade, "Broadly tunable vacuum-ultraviolet radiation source employing resonant enhanced sum-difference frequency mixing in krypton," J. Opt. Soc. Am. B **7**, 1254–1259 (1990).
16. I. D. Setija, H. G. C. Werij, O. J. Luiten, M. W. Reynolds, T. W. Hijmans, and J. T. Walraven, "Optical cooling of atomic hydrogen in a magnetic trap," Phys. Rev. Lett. **70**, 2257–2260 (1993).
17. K. S. E. Eikema, J. Walz, and T. W. Hänsch, "Continuous wave coherent Lyman-α radiation," Phys. Rev. Lett. **83**, 3828–3831 (1999).
18. M. Scheid, D. Kolbe, F. Markert, T. W. Hänsch, and J. Walz, "Continuous-wave Lyman-α generation with solid-state lasers," Opt. Express **17**, 11274–11280 (2009).
19. J. J. McClelland and M. H. Kelley, "Detailed look at aspects of optical pumping in sodium," Phys. Rev. A **31**, 3704–3710 (1985).
20. G. Avila, V. Giordano, V. Candelier, E. de Clercq, G. Theobald, and P. Cerez, "State selection in a cesium beam by laser-diode optical pumping," Phys. Rev. A **36**, 3719–3728 (1987).
21. P. Dalmas de Réotier and A. Yaouanc, "Muon spin rotation and relaxation in magnetic materials," J. Phys. Condens. Matter **9**, 9113–9166 (1997).
22. P. Strasser, K. Nagamine, T. Matsuzaki, K. Ishida, Y. Matsuda, K. Itahashi, and M. Iwasaki, "Muon spectroscopy with unstable nuclei," J. Phys. G **29**, 2047–2049 (2003).
23. J. P. Miller, E. de Rafael, and B. L. Roberts, "Muon (g-2) experiment and theory," Rep. Prog. Phys. **70**, 795–881 (2007).
24. S. Nagamiya, K. Nagamine, O. Hashimoto, and T. Yamazaki, "Negative-muon spin rotation at the oxygen site in paramagnetic MnO^{+}," Phys. Rev. Lett. **35**, 308–311 (1975).
25. P. Bakule, Y. Matsuda, Y. Miyake, P. Straser, K. Shimomura, S. Makimura, and K. Nagamine, "Slow muon experiment by laser resonant ionization method at RIKEN-RAL muon facility," SSpectrochim. Acta, B At. Spectrosc. **58**, 1019–1030 (2003).
26. P. Bakule and E. Morenzoni, "Generation and application of slow polarized muons," Contemp. Phys. **45**, 203–225 (2004).
27. T. Nakajima and N. Yonekura, "Electron spin-polarized alkaline-earth ions produced by multiphoton ionization," J. Chem. Phys. **117**, 2112–2119 (2002).
28. T. Nakajima, N. Yonekura, Y. Matsuo, T. Kobayashi, and Y. Fukuyama, "Simultaneous production of spin-polarized ions/electrons based on two-photon ionization of laser-ablated metallic atoms," Appl. Phys. Lett. **83**, 2103–2105 (2003).
29. N. Yonekura, T. Nakajima, Y. Matsuo, T. Kobayashi, and Y. Fukuyama, "Electron-spin polarization of photoions produced through photoionization from the laser-excited triplet state of Sr," J. Chem. Phys. **120**, 1806–1812 (2004).
30. T. Nakajima, "Control of the spin-polarization of photoelectrons/photoions using short laser pulses," Appl. Phys. Lett. **84**, 3786–3788 (2004).
31. T. Nakajima, "Effects of laser intensity and applied electric field on coherent control of spin polarization by short laser pulses," Appl. Phys. Lett. **88**, 111105–111107 (2006).
32. T. Nakajima, Y. Matsuo, and T. Kobayashi, "All-optical control and direct detection of ultrafast spin polarization in a multi-valence-electron system," Phys. Rev. A **77**, 063404 (2008).
33. T. Nakajima, "Investigation of ultrafast nuclear spin polarization induced by short laser pulses," Phys. Rev. Lett. **99**, 024801 (2007).
34. T. Nakajima, "Ultrafast nuclear spin polarization for isotopes with large nuclear spin," J. Opt. Soc. Am. B **26**, 572–580 (2009).
35. H. J. Andra, H. J. Plohn, A. Gaupp, and R. Frohling, "Nuclear-spin polarization produced by ion-beam-surface-interaction, its optical detection and use in an atomic quantum-beat experiment," Z. Phys. A **281**, 15–20 (1977).
36. C. Fabre, M. Gross, and S. Haroche, "Determination by quantum beat spectroscopy of fine-structure intervals in a series of highly excited sodium *D* states," Opt. Commun. **13**, 393–397 (1975).
37. J. S. Deech, R. Luypaert, and G. W. Series, "Determination of lifetimes and hyperfine structures of 8,9 and 10 $^2D_{3/2}$ states of ^{133}Cs by quantum-beat spectroscopy," J. Phys. B **8**, 1406–1414 (1975).
38. E. Sokell, S. Zamith, M. A. Bouchene, and B. Girard, "Polarization-dependent pump-probe studies in atomic fine-structure levels: towards the production of spin-polarized electrons," J. Phys. B **33**, 2005–2015 (2000).
39. M. A. Bouchene, S. Zamith, and B. Girard, "Spin-polarized electrons produced by a sequence of two femtosecond pulses. Calculation of differential and global polarization rates," J. Phys. B **34**, 1497–1512 (2001).

#135117 - $15.00 USD Received 14 Sep 2010; revised 2 Nov 2010; accepted 9 Dec 2010; published 14 Dec 2010

40. E. Takahashi, Y. Nabekawa, and K. Midorikawa, "Generation of 10-μJ coherent extreme-ultraviolet light by use of high-order harmonics," Opt. Lett. **27**, 1920–1922 (2002).
41. W. B. Westerveld, K. Becker, P. W. Zetner, J. J. Corr, and J. W. McConkey, "Production and measurement of circular polarization in the VUV," Appl. Opt. **24**, 2256–2262 (1985).
42. T. Koide, T. Shidara, M. Yuri, N. Kandaka, and H. Fukutani, "Production and direct measurement of circularly polarized vacuum-ultraviolet light with multireflection optics," Appl. Phys. Lett. **58**, 2592–2594 (1991).
43. H. Höchst, R. Patel, and F. Middleton, "Multiple-reflection $\lambda/4$ phase shifter: a viable alternative to generate circular-polarized synchrotron radiation," Nucl. Instrum. Methods Phys. Res. A **347**, 107–114 (1994).
44. L. Museur, C. Olivero, D. Riedel, and M. C. Castex, "Polarization properties of coherent VUV light at 125 nm generated by sum-frequency four-wave mixing in mercury," Appl. Phys. B **70**, 499–503 (2000).
45. R. Irrgang, M. Drescher, F. Gierschner, M. Spieweck, and U. Heinzmann, "A laser light source for circularly polarized VUV radiation," Meas. Sci. Technol. **9**, 422–427 (1998).

1. Introduction

There is a great demand to polarize *unstable* nuclei in nuclear physics [1]. Certainly the time scale to accomplish nuclear-spin polarization must be shorter than the lifetime of unstable nuclei. Among others the most well-known methods to polarize nuclei are nuclear-fragmentation method, optical pumping by a continuous-laser [2–8], and a combination of optical pumping and spin-exchange collisions [9, 10].

If a level structure of the target is simple and a powerful light source in a continuous mode is available, optical pumping may be efficiently used to polarize nuclei. How fast the nuclear-spin polarization is realized by optical pumping crucially depends on the intensity of the pump laser, lifetime of the upper state, and the corresponding dipole moment. Namely, if the pump intensity is low, a very long interaction time is required and vice versa, since a low intensity means that only a very small fraction of atoms in the ground state is pumped to the excited state, after which the spontaneous decay takes place back to the ground state. More precisely, it can be said that, for the optical pumping technique to work, the *pulse area*, which is a dimensionless quantity associated with the time-integration of the corresponding Rabi frequency, must be sufficiently large. Unfortunately, if the pumping wavelength becomes shorter and falls into the vacuum-ultraviolet (VUV) region, it would be very difficult to obtain a light source with a sufficient brightness. That is indeed the case of the muonium (μ^+e^-) and hydrogen atom, etc. for which the pumping wavelength is about 122 nm (Lyman-α line). In particular polarizing the muonium is a very challenging task because its lifetime is only 2.2 μs.

Historically the generation of a (tunable) light source for the Lyman-α line has been an important issue [11–18], since such a light source is invaluable for the plasma diagnosis and precision spectroscopy of hydrogen, etc. So far the reported Lyman-α light sources are generated in the continuous-wave (CW) [17, 18] or nanosecond pulsed mode [11–16] by combining different nonlinear optical processes. Although the operation of the Lyman-α light source in the CW or ns pulsed mode is essential to obtain a narrowband radiation, the efficiency to generate the Lyman-α radiation is usually very low.

The purpose of this paper is to show that a sequence of short laser pulses can efficiently realize nuclear-spin polarization within the time scale of a few to tens of ns. This is a variant of the optical pumping technique with an important difference that a pump laser is in the pulsed (ps or fs) mode instead of a CW mode. We emphasize that there are two big advantages of using short laser pulses for optical pumping, in particular in the VUV range. First, the use of intense short laser pulses increases the efficiency of nonlinear frequency conversion processes compared with those of CW lasers and ns lasers. Second, the spectral bandwidth of short laser pulses is extremely broad compared with those of CW and ns lasers, and hence we do not have to make efforts to match the laser spectral profile with all hyperfine transitions of the target atom for the efficient pumping. It is, however, far from obvious how much nuclear-spin polarization we can achieve with a sequence of short laser pulses under realistic pumping conditions.

#135117 - $15.00 USD Received 14 Sep 2010; revised 2 Nov 2010; accepted 9 Dec 2010; published 14 Dec 2010

To rigorously describe such unusual situations for optical pumping, we employ a quantum mechanical description of the system through a set of density matrix equations [19], since the standard treatment of optical pumping with a CW laser in terms of rate equations [20] fails.

In this paper we present a specific example for the muonium. Polarized muon is of great interest [21–23] for many years. For instance, spin-polarized (positive) muons are a powerful tool to probe the magnetic properties of the target and the technique is called muon spin rotation and relaxation (μSR) [21,24]. However, the kinetic energy of the muon beam produced through the decay of pions is in a few tens of MeV and they go deep (mm order) into the sample. In order to probe the magnetic property of the sample very near the surface (μm$\sim$nm order), an ultraslow muon beam with high spin-polarization is necessary [25, 26], which is a very demanding task.

Related to the present work, we have proposed a few different schemes to realize spin-polarization of electrons/ions [27–32] and nuclei [33, 34] using laser pulses. Essentially speaking, we can classify our polarization schemes into two kinds, neither of which, however, utilizes the so-called optical pumping technique, and hence completely different from the present scheme. In the first kind, the fine structure of atoms is spectrally resolved by the ns pump pulse and ionization is induced by the ns probe pulse. This implies that ionization takes place from the spin-resolved fine structure state, and therefore we can expect spin-polarization in photoelectrons as well as photoions, although how much spin-polarization we can indeed realize is not so simple. This is because the angular momentum of photons from circularly-polarized pump or probe pulses is redistributed between the spin and orbital angular momenta of photoelectrons as well as photoions. We have experimentally demonstrated spin-polarization of Sr atoms using ns pump and probe pulses [28]. In the second kind, the fine structure of the excited state is not spectrally resolved by the short pump pulse, implying that a coherent superposition of the corresponding manifold is produced. After the short pump pulse, coherence evolves in time in terms of the spin precession under the field-free condition, and the transient spin-polarization is realized for the electron-spin Needless to say, this is a variant of quantum beat [35–37] in a spin-resolved manner. An *indirect* signature of ultrafast spin-polarization has been reported for a one-electron atom, K, as a modulation of the (unpolarized) photoion signals [38, 39]. Using a two-valence-electron atom, Sr, we have successfully reported the *direct* experimental observation of unltrafast spin-polarization in the Sr^+ photoion signals, which agrees well with our *ab initio* theoretical prediction [32]. We have extended the idea to polarize nuclear-spin within the time-scale of a few to tens ns [33, 34], suggesting that even unstable nuclei can be highly polarized well within their lifetimes. Unfortunately the second kind of spin-polarization scheme does not work if the hyperfine splitting is too small and the natural lifetime is too short. As we will show later on in this paper, the present scheme works well under such situation, and therefore it is complementary to the second kind of spin-polarization scheme [33, 34].

2. Model

The relevant level diagram of the muonium atoms is shown in Fig. 1(a). Note that the muonium (μ^+e^-) atom has a very similar level structure with that of the hydrogen atom. The main difference between them can be seen in their hyperfine splittings. This comes from the extremely large magnetic moment of the muon compared with the proton. We assume that a sequence of laser pulses at a central photon energy of $\sim$10.2 eV with right-circular polarization coherently excites atoms in the ground $1s_{1/2}$ state to the excited $2p_{1/2}$ and $2p_{3/2}$ states which have a lifetime of 1.62 ns. Due to the presence of hyperfine interactions, each state splits into the two hyperfine levels, and Fig. 1(b) shows the level scheme of interest with all magnetic sublevels explicitly represented. Each pulse has been assumed to have a pulse duration, τ_L, defined for the full width at half maximum (FWHM) with a certain time interval, T, between them. Provided

#135117 - $15.00 USD Received 14 Sep 2010; revised 2 Nov 2010; accepted 9 Dec 2010; published 14 Dec 2010

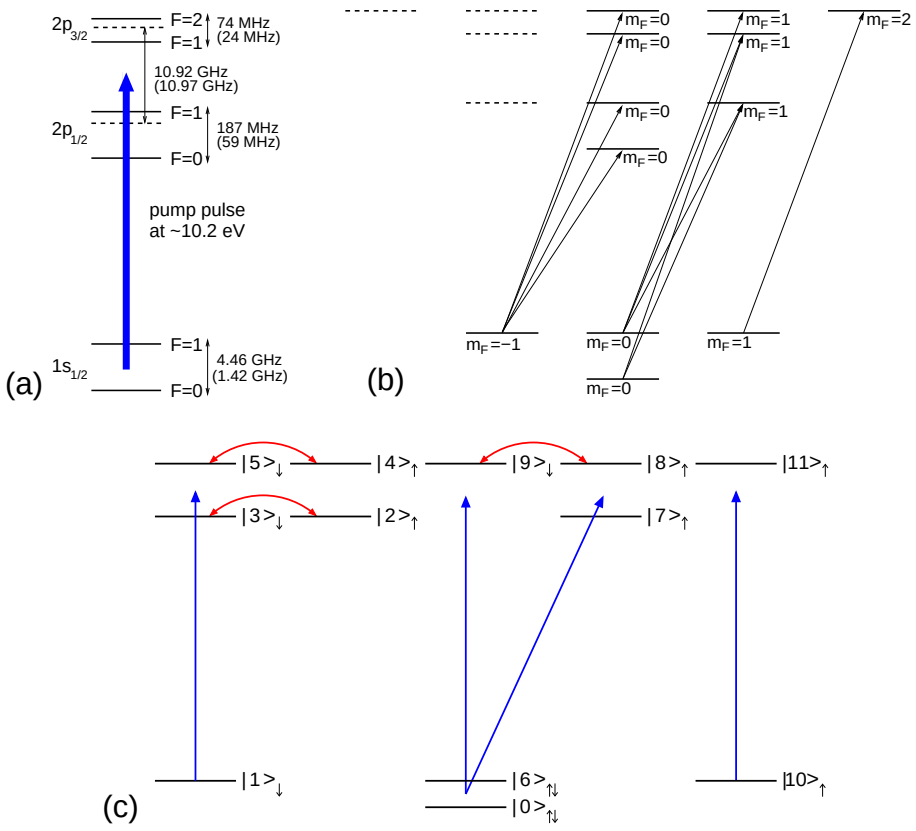

Fig. 1. (a) Level scheme. A sequence of right-circularly polarized short pulses pump the muonium (μ^+e) atoms in the ground $1s$ state to the $2p$ state. Energy values in the parentheses are those for the hydrogen atoms. (b) Level scheme with a clear distinction of magnetic sublevels. (c) Level scheme using the uncoupled basis for the excited states. Dipole interactions and hyperfine interactions in the excited states are depicted by the blue and red lines, respectively. The up and down arrows by the ket vectors represent the nuclear-spin orientations.

the peak field amplitude E_0, pulse duration τ_L, and number of pulses n_{max} with a time interval of T, the envelope function of the laser field reads

$$E(t) = E_0 \sum_{n=0}^{n_{max}} \exp\left[-2\ln 2\left(\frac{t-nT}{\tau_L}\right)^2\right] . \tag{1}$$

In this paper we assume that the duration of each pulse is 1 ps, i.e., $\tau_L = 1$ ps, which means that the spectral bandwidth of pump pulses is about 440 GHz. Clearly if the time interval between the pulses is in the time scale of a few to several ns, most atoms in the excited states go back to the ground state through the spontaneous decay before the next pulse arrives. Note that the dynamics of this system cannot be correctly described by rate equations, since they can account for neither the broad spectral bandwidth originating from the short pulse duration, Rabi oscillations, nor hyperfine interactions which can take place after the short laser pulses. We employ a set of density matrix equations to correctly account for the interaction dynamics. A special care, however, has to be taken for the present case where the hyperfine coupling time is comparable to the lifetime of the $2p$ state. Namely the use of the coupled basis

#135117 - $15.00 USD Received 14 Sep 2010; revised 2 Nov 2010; accepted 9 Dec 2010; published 14 Dec 2010

represented by $|(((ls)\,j)I)FM_F\rangle$ is not very convenient to correctly describe the entire process. Instead we use the uncoupled basis description, $|((ls)\,j)M_j\rangle|IM_I\rangle$, for the excited states. For simplicity, we will drop I in $|IM_I\rangle$ from now on. Now the relevant level scheme with the uncoupled basis states employed for the excited states are shown in Fig. 1(c), where the following notations for the states of interests have been introduced: $|0\rangle = |(1s_{1/2})\,F=0\,M_F=0\rangle$, $|1\rangle = |(1s_{1/2})\,F=1\,M_F=-1\rangle$, $|2\rangle = |(2p_{1/2})\,M_J=-1/2\rangle|M_I=1/2\rangle$, $|3\rangle = |(2p_{1/2})\,M_J=1/2\rangle|M_I=-1/2\rangle$, $|4\rangle = |(2p_{3/2})\,M_J=-1/2\rangle|M_I=1/2\rangle$, $|5\rangle = |(2p_{3/2})\,M_J=1/2\rangle|M_I=-1/2\rangle$, $|6\rangle = |(1s_{1/2})\,F=1\,M_F=0\rangle$, $|7\rangle = |(2p_{1/2})\,M_J=1/2\rangle|M_I=1/2\rangle$, $|8\rangle = |(2p_{3/2})\,M_J=1/2\rangle|M_I=1/2\rangle$, $|9\rangle = |(2p_{3/2})\,M_J=3/2\rangle|M_I=-1/2\rangle$, $|10\rangle = |(1s_{1/2})\,F=1\,M_F=1\rangle$, $|11\rangle = |(2p_{3/2})\,M_J=3/2\rangle|M_I=1/2\rangle$,

By inspection of Fig. 1(c) we can immediately see the advantage of the use of uncoupled basis description: For instance, consider the laser excitation from state $|1\rangle$. Since the nuclear-spin orientation of atoms in state $|1\rangle$ is 100 % spin-down and the dipole interaction does not work on nuclear-spin, the nuclear-spin orientation of atoms is unchanged just after the excitation by the short laser pulse. This is depicted by states $|3\rangle$ and $|5\rangle$ in Fig. 1(c), and clearly atoms in those states do not spontaneously decay to $|10\rangle$ since such a transition involves the change of nuclear-spin which is forbidden. Due to the presence of hyperfine coupling, however, the nuclear-spin flipping will periodically take place from $|3\rangle$ to $|2\rangle$ ($|5\rangle$ to $|4\rangle$) and vice versa, as represented by the red arrows in Fig. 1(c). In this way the laser excitation from $|1\rangle$ can populate not only the spin-unchanged states, $|3\rangle$ and $|5\rangle$, but also the spin-flipped states, $|2\rangle$ and $|4\rangle$, the spontaneous decay channels from which are different: a spontaneous decay from $|3\rangle$ will end up with $|0\rangle$, $|1\rangle$, and $|6\rangle$ with the branching ratio of 1:4:1, while that from $|2\rangle$ will end up with $|0\rangle$, $|6\rangle$, and $|10\rangle$ with the branching ratio of 1:1:4. Clearly the hyperfine couplings in the excited states help polarize the nuclei. Another important remark is that, although the hyperfine couplings in the excited states help polarize the nuclei, our scheme still works even if the hyperfine couplings in the excited states are very weak, because the hyperfine couplings still take place in the lower (ground) states during the time interval between the pulses. Recall that the hyperfine coupling time of the ground state is sub-ns for the muonium, while the time interval between the pulses is assumed to be several ns in this paper.

For the quantitative description of the time-dependent dynamics of nuclear-spin, we must numerically solve a set of density matrix equations. We start from the equation of motion of the density operator, ρ, i.e., $i\hbar\dot{\rho} = [\mathscr{H}_0 + \mathscr{H}_1 + D, \rho]$, where $\mathscr{H}_0$ is the unperturbed atomic Hamiltonian *excluding* the hyperfine interactions among the excited states, $\mathscr{H}_1$ is the hyperfine interactions among the excited state, and D is a electric dipole operator. Namely it is $\mathscr{H}_0 + \mathscr{H}_1$ that represents the total unperturbed atomic Hamiltonian. This is a convenient definition of the total unperturbed atomic Hamiltonian, since we have introduced the uncoupled basis description to describe the excited states and therefore the hyperfine interactions in the excited states must be treated separately. Using the basis set, $\{|j\rangle\}$ $(j = 0, 1, ..., 11)$, we can obtain all density matrix elements by calculating $\dot{\rho}_{ij} = -i\hbar^{-1}\sum_k(\mathscr{H}_{ik}\rho_{kj} - \rho_{ik}\mathscr{H}_{kj})$. After introducing the rotating-wave approximation and phenomenologically adding the spontaneous decay terms, we finally obtain the set of equations for the density matrix elements, σ_{ij} $(i, j = 0, 1, ..., 11)$, which reads

$$\dot{\sigma}_{00} = \gamma_{sp}(\frac{1}{6}\sigma_{22} + \frac{1}{6}\sigma_{33} + \frac{1}{3}\sigma_{44} + \frac{1}{3}\sigma_{55} + \frac{1}{3}\sigma_{77} + \frac{1}{6}\sigma_{88} + \frac{1}{2}\sigma_{99}) - i\sum_{k=7,8,9}\Omega_{0k}(\sigma_{k0} - \sigma_{0k})\,, \quad (2)$$

$$\dot{\sigma}_{11} = \gamma_{sp}(\frac{2}{3}\sigma_{33} + \frac{1}{3}\sigma_{55}) - i\Omega_{13}(\sigma_{31} - \sigma_{13}) - i\Omega_{15}(\sigma_{51} - \sigma_{15})\,, \quad (3)$$

$$\dot{\sigma}_{22} = -\gamma_{sp}\sigma_{22} - i\Omega_{32}^{(H)}(\sigma_{32} - \sigma_{23})\,, \quad (4)$$

#135117 - $15.00 USD Received 14 Sep 2010; revised 2 Nov 2010; accepted 9 Dec 2010; published 14 Dec 2010

$$\dot{\sigma}_{33} = -\gamma_{sp}\sigma_{33} + i\Omega_{32}^{(H)}(\sigma_{32} - \sigma_{23}) + i\Omega_{13}(\sigma_{31} - \sigma_{13}) \,, \tag{5}$$

$$\dot{\sigma}_{44} = -\gamma_{sp}\sigma_{44} - i\Omega_{54}^{(H)}(\sigma_{54} - \sigma_{45}) \,, \tag{6}$$

$$\dot{\sigma}_{55} = -\gamma_{sp}\sigma_{55} + i\Omega_{54}^{(H)}(\sigma_{54} - \sigma_{45}) + i\Omega_{15}(\sigma_{51} - \sigma_{15}) \,, \tag{7}$$

$$\dot{\sigma}_{66} = \gamma_{sp}(\frac{1}{6}\sigma_{22} + \frac{1}{6}\sigma_{33} + \frac{1}{3}\sigma_{44} + \frac{1}{3}\sigma_{55} + \frac{1}{3}\sigma_{77} + \frac{1}{6}\sigma_{88} + \frac{1}{2}\sigma_{99}) - i\sum_{k=7,8,9}\Omega_{6k}(\sigma_{k6} - \sigma_{6k}) \,, \tag{8}$$

$$\dot{\sigma}_{77} = -\gamma_{sp}\sigma_{77} + i\Omega_{07}(\sigma_{70} - \sigma_{07}) + i\Omega_{67}(\sigma_{76} - \sigma_{67}) \,, \tag{9}$$

$$\dot{\sigma}_{88} = -\gamma_{sp}\sigma_{88} - i\Omega_{98}^{(H)}(\sigma_{98} - \sigma_{89}) + i\Omega_{08}(\sigma_{80} - \sigma_{08}) + i\Omega_{68}(\sigma_{86} - \sigma_{68}) \,, \tag{10}$$

$$\dot{\sigma}_{99} = -\gamma_{sp}\sigma_{99} + i\Omega_{98}^{(H)}(\sigma_{98} - \sigma_{89}) + i\Omega_{09}(\sigma_{90} - \sigma_{09}) + i\Omega_{69}(\sigma_{96} - \sigma_{69}) \,, \tag{11}$$

$$\dot{\sigma}_{1010} = \gamma_{sp}(\frac{2}{3}\sigma_{22} + \frac{1}{3}\sigma_{44} + \frac{1}{3}\sigma_{77} + \frac{2}{3}\sigma_{88} + \sigma_{1111}) - i\Omega_{1011}(\sigma_{1110} - \sigma_{1011}) \,, \tag{12}$$

$$\dot{\sigma}_{1111} = -\gamma_{sp}\sigma_{1111} + i\Omega_{1011}(\sigma_{1110} - \sigma_{1011}) \,, \tag{13}$$

$$\dot{\sigma}_{60} = -i\omega_{60}\sigma_{60} - i\sum_{j=7\,to\,9}\Omega_{6j}\sigma_{j0} + i\sum_{j=7,9}\Omega_{j0}\sigma_{6j} \,, \tag{14}$$

$$\dot{\sigma}_{70} = (i\Delta_{70} - \frac{\gamma_{sp}}{2})\sigma_{70} + i\Omega_{70}(\sigma_{77} - \sigma_{00}) - i\Omega_{76}\sigma_{60} + i\Omega_{80}\sigma_{78} + i\Omega_{90}\sigma_{79} \,, \tag{15}$$

$$\dot{\sigma}_{80} = (i\Delta_{80} - \frac{\gamma_{sp}}{2})\sigma_{80} - i\Omega_{89}^{(H)}\sigma_{90} + i\Omega_{80}(\sigma_{88} - \sigma_{00}) - i\Omega_{86}\sigma_{60} + i\Omega_{70}\sigma_{87} + i\Omega_{90}\sigma_{89} \,, \tag{16}$$

$$\dot{\sigma}_{90} = (i\Delta_{90} - \frac{\gamma_{sp}}{2})\sigma_{90} - i\Omega_{98}^{(H)}\sigma_{80} + i\Omega_{90}(\sigma_{99} - \sigma_{00}) - i\Omega_{96}\sigma_{60} + i\Omega_{70}\sigma_{97} + i\Omega_{80}\sigma_{98} \,, \tag{17}$$

$$\dot{\sigma}_{21} = (i\Delta_{21} - \frac{\gamma_{sp}}{2})\sigma_{21} - i\Omega_{23}^{(H)}\sigma_{31} + i\Omega_{31}\sigma_{23} + i\Omega_{51}\sigma_{25} \,, \tag{18}$$

$$\dot{\sigma}_{31} = (i\Delta_{31} - \frac{\gamma_{sp}}{2})\sigma_{31} - i\Omega_{32}^{(H)}\sigma_{21} + i\Omega_{31}(\sigma_{33} - \sigma_{11}) + i\Omega_{51}\sigma_{35} \,, \tag{19}$$

$$\dot{\sigma}_{41} = (i\Delta_{41} - \frac{\gamma_{sp}}{2})\sigma_{41} - i\Omega_{45}^{(H)}\sigma_{51} + i\Omega_{31}\sigma_{43} + i\Omega_{51}\sigma_{45} \,, \tag{20}$$

$$\dot{\sigma}_{51} = (i\Delta_{51} - \frac{\gamma_{sp}}{2})\sigma_{51} - i\Omega_{54}^{(H)}\sigma_{41} + i\Omega_{51}(\sigma_{55} - \sigma_{11}) + i\Omega_{31}\sigma_{53} \,, \tag{21}$$

$$\dot{\sigma}_{32} = -\gamma_{sp}\sigma_{32} + i\Omega_{23}^{(H)}(\sigma_{33} - \sigma_{22}) - i\Omega_{31}\sigma_{12} \,, \tag{22}$$

#135117 - $15.00 USD Received 14 Sep 2010; revised 2 Nov 2010; accepted 9 Dec 2010; published 14 Dec 2010

$$\dot{\sigma}_{42} = (-\omega_{42} - \gamma_{sp})\sigma_{42} - i\Omega_{45}^{(H)}\sigma_{52} + i\Omega_{32}^{(H)}\sigma_{43} \,, \tag{23}$$

$$\dot{\sigma}_{52} = (-\omega_{52} - \gamma_{sp})\sigma_{52} - i\Omega_{54}^{(H)}\sigma_{42} + i\Omega_{32}^{(H)}\sigma_{53} - i\Omega_{51}\sigma_{12} \,, \tag{24}$$

$$\dot{\sigma}_{43} = (-i\omega_{43} - \gamma_{sp})\sigma_{43} - i\Omega_{45}^{(H)}\sigma_{53} + i\Omega_{23}^{(H)}\sigma_{42} + i\Omega_{13}\sigma_{41} \,, \tag{25}$$

$$\dot{\sigma}_{53} = (-i\omega_{53} - \gamma_{sp})\sigma_{53} - i\Omega_{54}^{(H)}\sigma_{43} + i\Omega_{23}^{(H)}\sigma_{52} - i\Omega_{51}\sigma_{13} + i\Omega_{13}\sigma_{51} \,, \tag{26}$$

$$\dot{\sigma}_{54} = -\gamma_{sp}\sigma_{54} + i\Omega_{54}^{(H)}(\sigma_{55} - \sigma_{44}) - i\Omega_{51}\sigma_{14} \,, \tag{27}$$

$$\dot{\sigma}_{76} = (-i\Delta_{76} - \frac{\gamma_{sp}}{2})\sigma_{76} + i\Omega_{76}(\sigma_{77} - \sigma_{66}) - i\Omega_{70}\sigma_{06} + i\Omega_{86}\sigma_{78} + i\Omega_{96}\sigma_{79} \,, \tag{28}$$

$$\dot{\sigma}_{86} = (-i\Delta_{86} - \frac{\gamma_{sp}}{2})\sigma_{86} - i\Omega_{89}^{(H)}\sigma_{96} + i\Omega_{86}(\sigma_{88} - \sigma_{66}) - i\Omega_{80}\sigma_{06} + i\Omega_{76}\sigma_{87} + i\Omega_{96}\sigma_{89} \,, \tag{29}$$

$$\dot{\sigma}_{96} = (-i\Delta_{96} - \frac{\gamma_{sp}}{2})\sigma_{96} - i\Omega_{98}^{(H)}\sigma_{86} + i\Omega_{96}(\sigma_{99} - \sigma_{66}) - i\Omega_{90}\sigma_{06} + i\Omega_{76}\sigma_{97} + i\Omega_{86}\sigma_{98} \,, \tag{30}$$

$$\dot{\sigma}_{87} = (-i\omega_{87} - \gamma_{sp})\sigma_{87} - i\Omega_{89}^{(H)}\sigma_{97} - i\Omega_{80}\sigma_{07} - i\Omega_{86}\sigma_{67} + i\Omega_{07}\sigma_{80} + i\Omega_{67}\sigma_{86} \,, \tag{31}$$

$$\dot{\sigma}_{97} = (-i\omega_{97} - \gamma_{sp})\sigma_{97} - i\Omega_{98}^{(H)}\sigma_{87} - i\Omega_{90}\sigma_{07} - i\Omega_{96}\sigma_{67} + i\Omega_{07}\sigma_{90} + i\Omega_{67}\sigma_{96} \,, \tag{32}$$

$$\dot{\sigma}_{98} = -\gamma_{sp}\sigma_{98} + i\Omega_{98}^{(H)}(\sigma_{99} - \sigma_{88}) - i\Omega_{90}\sigma_{08} - i\Omega_{96}\sigma_{68} + i\Omega_{08}\sigma_{90} + i\Omega_{68}\sigma_{96} \,, \tag{33}$$

$$\dot{\sigma}_{1110} = (-\Delta_{1110} - \frac{\gamma_{sp}}{2})\sigma_{1110} + i\Omega_{1110}(\sigma_{1111} - \sigma_{1010}) \,, \tag{34}$$

where Ω_{ij} is a Rabi frequency and defined as $\Omega_{ij} = \mu_{ij}E(t)/\hbar$ with μ_{ij} being a dipole moment between $|i\rangle$ and $|j\rangle$.

Similarly $\Omega_{ij}^{(H)}$ is a non-radiative hyperfine coupling between states $|i\rangle$ and $|j\rangle$, which is defined as $\Omega_{ij}^{(H)} = |\omega_{ij}|/2$ with $\omega_{ij} = \omega_i - \omega_j$. γ_{sp} represents a spontaneous decay rate which are exactly the same for all excited hyperfine states of both hydrogen and muonium. Δ_{ij} is the detuning defined as $\Delta_{ij} = \omega - \omega_{ij}$ where ω is the central photon energy. The branching coefficients of the spontaneous decay such as those appearing in Eqs. (2), (3), (8), and (12) simply arise from the ratios of the Clebsh-Gordan coefficients of the relevant transition matrix elements.

Now, with the pulse function given by Eq. (1), we numerically solve Eqs. (2)–(34) for different peak intensities, time intervals, number of pulses, and laser detunings with an initial condition, for a moment, that the four ground hyperfine states of $1s_{1/2}$ with $F = 0$ and $F = 1$ are equally populated before the laser pulses, i.e., $\sigma_{00} = \sigma_{11} = \sigma_{66} = \sigma_{1010} = 1/4$ at $t = -\infty$. Since we are interested in nuclear-spin polarization after all atoms in the excited hyperfine states

#135117 - $15.00 USD Received 14 Sep 2010; revised 2 Nov 2010; accepted 9 Dec 2010; published 14 Dec 2010

spontaneously decay back to the four ground hyperfine states, the degree of spin-polarization, P, is defined for atoms in the ground state using the relation of

$$P = \frac{P_{up} - P_{down}}{P_{up} + P_{down}} , \tag{35}$$

where

$$P_{up} = \frac{1}{2}\sigma_{00}(t=\infty) + \frac{1}{2}\sigma_{66}(t=\infty) + \sigma_{1010}(t=\infty) \tag{36}$$

and

$$P_{down} = \frac{1}{2}\sigma_{00}(t=\infty) + \sigma_{11}(t=\infty) + \frac{1}{2}\sigma_{66}(t=\infty) . \tag{37}$$

In Eqs. (36) and (37), P_{up} and P_{down} represent the population of muonium atoms in the ground state with up and down nuclear-spin, respectively.

Before we move on to show representative numerical results, we would like to make some remarks on the generation of a sequence of right-circularly polarized 10.2 eV pulses with a ps duration and sufficient pulse energy for the practical applicability of our scheme. The experimental setup we propose is described in Fig. 2: We can use a pulse stacking technique to obtain

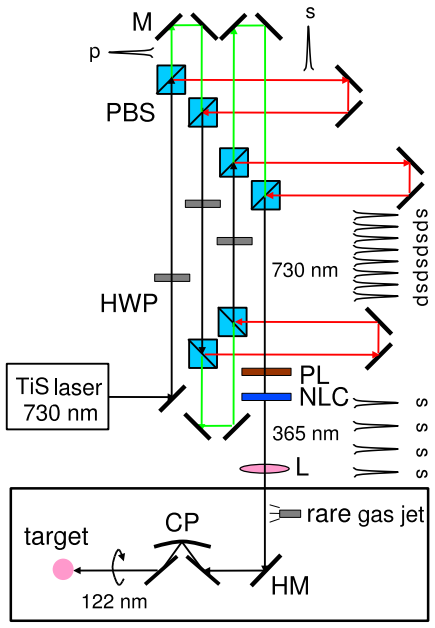

Fig. 2. Proposed experimental setup. Starting from a ps Ti:Sapphire laser tuned at 730 nm, a three-stage pulse stacker produces 8 pulses with alternating (s- and p-) linear polarization. A polarizer picks up one of the polarization components of the pulses to produce the second-harmonic by a nonlinear crystal. The 365 nm pulses interact with rare gas atoms to produce the third-harmonic at 122 nm ($\sim$10.2 eV). A circular polarizer (CP) appropriately tilted around the optical axis converts its polarization from linear to circular to pump the target atoms. HWP, PBS, PL, NLC, L, and HM stand for a half-wave plate, polarizing beam splitter, linear polarizer, nonlinear crystal, focusing lens, and harmonic mirror, respectively.

#135117 - $15.00 USD Received 14 Sep 2010; revised 2 Nov 2010; accepted 9 Dec 2010; published 14 Dec 2010

a sequence of pulses from a single ps Ti:Sapphire laser pulse at 730 nm. If we employ a m-stage pulse stacking, the number of pulses we obtain is 2^m ($m = 3$ in Fig. 2) with alternative linear polarization, s and p. With the use of a linear polarizer we pick up pulses with p-polarization only, and the number of pulses is now 2^{m-1}, resulting in the energy throughput of about 50 %. The 730 nm pulses are now converted to the 365 nm pulses with a nonlinear crystal. Using those pulses at 365 nm, we produce a sequence of 122 nm ($\sim$ 10.2 eV) pulses through the third-harmonic generation.

Alternatively, if one uses Ti:Sapphire laser pulses tuned at 851 nm, the 10.2 eV pulses may be produced as the 7^{th} harmonic. High-order harmonic generation (HHG) is a well-studied process, and the pulse energies of the HHG can be as much as 6, 4, and 1 μJ for the 11^{th}, 13^{rd}, and 15^{th} harmonics [40], respectively. We expect much more pulse energy for the 7^{th} harmonic, since it is a lower order harmonic. The 10.2 eV pulses produced by the above prescription have linear (s-) polarization. We must now change polarization of the 10.2 eV pulses from linear to circular. This can be done by the use of a circular polarizer [41–43] with a transmission of about 5-10 %. Another way of producing circularly polarized 122 nm pulses is to use a combination of linearly and circularly polarized 365 nm pulses to *directly* produce 122 nm pulses with circular polarization by sum-frequency four-wave mixing [44, 45], which is in our case third-harmonic generation. Such a scheme is more complicated to prepare the 365 nm pulses but can be more advantageous to avoid the order-of-magnitude energy loss by the use of a circular polarizer. A simple estimation shows that a 1 ps pulse at 10.2 eV photon energy with a pulse energy of 10 μJ results in the peak intensity of 1.3×10^9 W/cm^2 if the beam diameter is 1 mm.

Of course, depending on the kind of target atoms to be polarized, we may not need laser pulses in the VUV range. In such a case, we can replace the harmonic generation arrangement in Fig. 2 by other kind of frequency-conversion arrangement and the experimental setup becomes much simpler.

3. Results and discussions

Now we present representative numerical results. First we consider the case of a *single* pump pulse. In Fig. 3 we show the variation of spin-polarization as a function of detuning with dif-

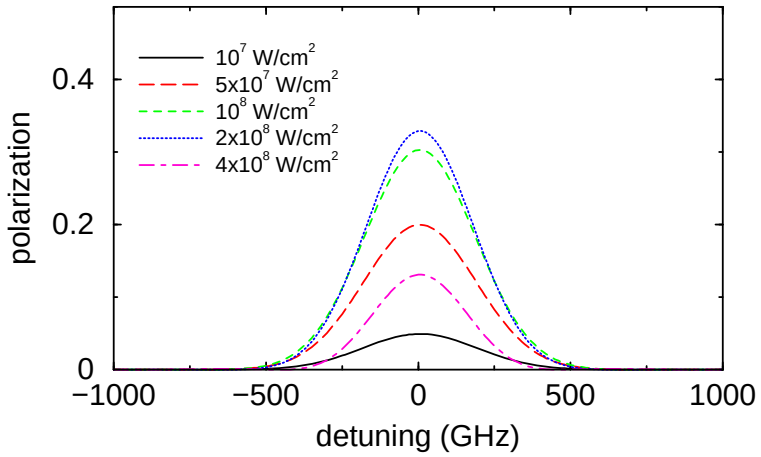

Fig. 3. Polarization after interacting with a single pump pulse as a function of detuning. Solid, long-dashed, dashed, dotted, and dot-dashed curves represent the employed peak intensities, which are 10^7, 5×10^7, 10^8, 2×10^8, and 4×10^8 W/cm^2, respectively.

#135117 - $15.00 USD Received 14 Sep 2010; revised 2 Nov 2010; accepted 9 Dec 2010; published 14 Dec 2010

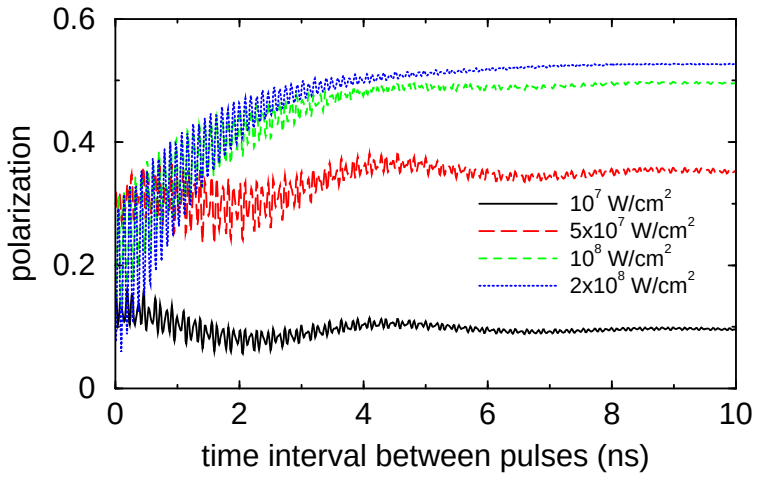

Fig. 4. Polarization after interacting with two pump pulses as a function of time interval between the two pulses. Solid, long-dashed, dashed, and dotted curves represent the employed peak intensities, which are 10^7, 5×10^7, 10^8, and 2×10^8 W/cm^2, respectively.

ferent peak intensities where zero detuning means that the 10.2 eV pump pulse is on resonant with the $1s_{1/2}$ $(F=1)$-$2p_{1/2}$ $(F=0)$ hyperfine transition. Positive (negative) detunings imply that the photon energy is larger (smaller) than this. As the peak intensity increases the degree of spin-polarization increases up to 2×10^8 W/cm^2 where the pulse area is already a bit more than π and nearly-complete population inversion takes place. If we further increase the peak intensity, for instance 4×10^8 W/cm^2, the degree of spin-polarization starts to decrease because the *effective* pulse area (modulus of π) becomes smaller. Note that it is an effective pulse area and not the pulse area that matters. It is clear that we have no reason to make the peak intensity of each pulse higher than 2×10^8 W/cm^2.

Now we consider the case of *two* pulses. Change of spin-polarization for the different peak intensities and the detunings are shown in Fig. 4 as a function of time interval between the pulses. The detuning has been set to be zero in this case. We note that the results are very similar even if we choose a little bit different detunings, $\pm$20GHz, due to the very broad laser bandwidth. We observe the presence of oscillations. Essentially they arise from the Ramsey interference in the time domain. In our case, however, we have a few different frequency components in the oscillations, since we are dealing with the multiple hyperfine transitions by short laser pulses with a very broad spectral bandwidth. Clearly the fastest oscillations are associated with the fine structure of $2p_{1/2}$ and $2p_{3/2}$, and hence $\sim$10.9 GHz. Because of the presence of hyperfine levels in $1s_{1/2}$, $2p_{1/2}$, and $2p_{3/2}$, there are a few slightly different frequency components which result in the slow modulation in Fig. 3. Naturally the influence of Ramsey interference becomes smaller for the larger time interval between the pulses due to the rapid loss of coherence through spontaneous decay, and at the 10 ns time interval the modulations are almost gone. We point out that the use of the two pump pulses improves the maximum degree of spin-polarization from $\sim$33 % for the single pulse to $\sim$53 % for the two pulses if we employ the peak intensity of 2×10^8 W/cm^2.

In Fig. 5 we show the temporal evolution of the degree of spin-polarization. for the case of five pulses with a fixed time interval of 5 ns. The detuning has been set to zero again. We see that the increment of the degree of spin-polarization after each pulse is approximately the same if the peak intensity is low, i.e., 10^7 W/cm^2. Indeed this situation is very similar to that

#135117 - $15.00 USD Received 14 Sep 2010; revised 2 Nov 2010; accepted 9 Dec 2010; published 14 Dec 2010

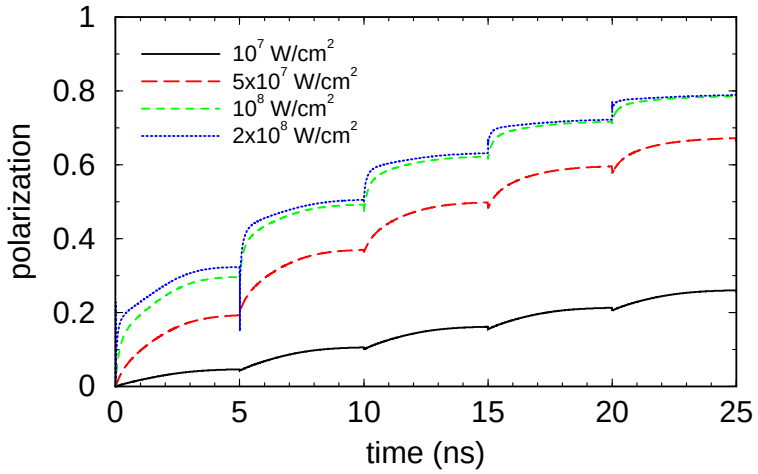

Fig. 5. Time evolution of polarization for different peak intensities. Solid, long-dashed, dashed, and dotted curves represent the employed peak intensities, which are 10^7, 5×10^7, 10^8, and 2×10^8 W/cm^2, respectively. The five 10.2 eV pulses are turned on at 0, 5, 10, 15, and 20 ns with a 5 ns time interval.

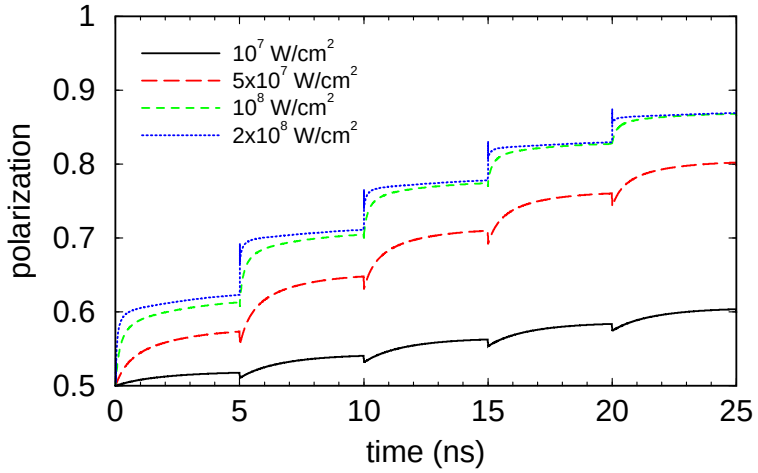

Fig. 6. Same with Fig. 5 but with the initial condition of 50 % spin-polarized before the pulses.

of the ordinary optical pumping by a CW laser. If the peak intensity is higher, however, the increment tends to become smaller as spin-polarization approaches unity. Our results clearly indicate that significant spin-polarization can be realized by using only a few 10.2 eV pulses with a ps duration and it can be as much as $\sim$80 % if the peak intensity is $\sim 10^8$ W/cm^2. The sharp decrease of polarization at the instant of laser pulses (5, 10, 15, 20, and 25 ns) for the peak intensities of 10^8 W/cm^2 and 2×10^8 W/cm^2 arises from the fact that we have defined the polarization only for atoms in the ground state: When the peak intensity is as high as 10^8 W/cm^2 and 2×10^8 W/cm^2, most atoms are in the excited states (almost complete population inversion), which results in the apparently irregular behavior of polarization defined for atoms in the ground state at the instant of laser pulses.

#135117 - $15.00 USD Received 14 Sep 2010; revised 2 Nov 2010; accepted 9 Dec 2010; published 14 Dec 2010

Upon production of muons they are known to be perfectly polarized. However, when they pick up electrons to become muonium atoms, the degree of polarization is reduced to about 50 %. An interesting question is how much we can increase the degree of spin-polarization with the present scheme. For that purpose we now change the initial condition and assume that $\sigma_{00} = \sigma_{66} = 1/4$, $\sigma_{1010} = 1/2$, and $\sigma_{11} = 0$ at $t = -\infty$. Results for the five pulses with a 5 ns time interval are presented in Fig. 6. Naturally a higher degree of spin-polarization can be achieved with this initial condition. According to our calculations (not shown here) we can achieve 94 % spin-polarization if we employ eight pulses with a 5 ns time interval.

4. Conclusions

In conclusion, we have shown that a sequence of short laser pulses can efficiently polarize nuclear-spin of atoms/ions. The scheme is very general and can be applicable to a variety of atoms/ions. This is a pulsed laser version of optical pumping and particularly useful when the lifetime of the target is very short and/or the pumping wavelength is too short to efficiently produce with a CW or ns laser. Since the short laser pulses have a very broad spectral bandwidth all hyperfine transitions as well as fine structure transitions are simultaneously excited. This, however, does not spoil the optical pumping processes. Indeed, our specific calculations for the unpolarized muonium atoms have shown that the degrees of spin-polarization can be as much as 33, 50, and 80 % by using a single, two, and five 10.2 eV pulses. If we can use eight pulses, it can be as much as 94 %.

Acknowledgement

The author acknowledges useful communications with Professor Yasuyuki Matsuda regarding the production and application of ultraslow muons. This work was supported by the Grant-in-Aid for scientific research from the Ministry of Education and Science of Japan.

#135117 - $15.00 USD Received 14 Sep 2010; revised 2 Nov 2010; accepted 9 Dec 2010; published 14 Dec 2010